

Effect of Alumina Substitution on Porosity and Thermal Expansion of Triaxial Porcelain-Like Bodies

M. Ghaffari¹, E. Salahi^{*2}, A. Rajabi²

¹Materials and Energy Research Center (MERC), P.O. Box 14155 – 4777, Karaj-Iran

²Department of Mechanical and Material Engineering, Faculty of Engineering & Built Environment Universiti Kebangsaan Malaysia, 43600 Bangi, UKM, Malaysia

received June 5, 2014; received in revised form July 15, 2014; accepted August 21, 2014

Abstract

Aluminous bodies are used in a wide variety of applications as a medium-strength ceramic. In this work, a full composition range of alumina, kaolin, and feldspar were fired at 1230 °C and 1400 °C, and were shown in a triaxial presentation, which can be used to make body calculations. Domestic kaolin has been studied for its potential as a raw material to produce aluminous bodies. The porosity and shrinkage of the samples were measured. When fired at 1400 °C, a wider composition range would result in porcelain-like bodies. The thermal expansion of the selected samples showed that the substitution of clay with alumina increased the thermal expansion coefficient. Firing at higher temperatures also affected thermal expansions in a similar manner.

Keywords: Triaxial bodies, thermal expansion, porosity

I. Introduction

Triaxial bodies consist of kaolin, quartz, and fluxes. Quartz as an inexpensive filler affects the thermal expansion of ceramic bodies. Bodies with higher quartz content have higher thermal expansion¹⁻³. A large difference exists between the thermal expansion of the quartz grains and the glass phase around them. The dissolution of SiO₂ decreases the thermal expansion of the glass phase, thus forming cracks around the quartz grains upon cooling, which in turn decreases its strength⁴⁻⁶. One of the main methods to increase the strength of triaxial bodies is the substitution of quartz with alumina. Although dissolution of Al₂O₃ lowers the thermal expansion of the glass phase around the alumina grains, it is not accompanied by high dimensional changes similar to quartz at 570 °C⁷⁻⁹. Elimination of cracks around the filler grains can cause a 100-% increase in strength, and the bending strength of porcelain increases as a function of alumina content up to 40%.^{1,10,11} Past literature^{12,13} has investigated the effect of the addition of alumina in whiteware bodies, and reported that this addition increases the strength caused by the lesser difference between the thermal expansions of the filler and glass phase around it. Iqbal *et al.*¹⁴ have re-studied the microstructure of aluminous porcelains and detected very fine mullite crystals around corundum grains, which grow as a result of the Al₂O₃ dissolution in the surrounding glass phase. They have quoted the other results that show an increase in the overall thermal expansion of bodies having up to 40 % alumina. The formation of mullite around the alumina grains has also been

confirmed by Carty and Senapati¹⁵. Traditional alumina bodies consists of 50 % to 60 % clay and equal amounts of alumina and flux. The flux consists of three parts feldspar and one part talc¹⁶. The influence of talc¹⁷ and BaCO₃¹⁸ on the microstructure, electrical, and mechanical properties of aluminous porcelain containing 20 % corundum has been studied.

The addition of talc reduces dielectric strength and modulus of rupture (MOR). The addition of BaCO₃, up to 1 %, increases the porosity and MOR, but further addition has no effect on these properties. The present work focuses on the influence of alumina substitution on the porosity and thermal expansion of triaxial bodies.

II. Experimental procedures

Domestic raw materials were used. The chemical and mineralogical analyses of raw materials are shown in Table 1.

Clay minerals were provided by SZWNK1 from Iran-China Clay Co. Quartz from the Hamedan region was used, and SF11 was from Setabran Co., which is purest potash feldspar available as flux. Alumina was provided by Jajarm mine and was purified by Iran Alumina Co. The particle size was measured by PSA Cilas 920. The samples were mixed in a slip, and were deflocculated using Dulapix CE64 from Zschimmer and Schwarz, which was effective on clayey and non-clay mixtures. The dewatering process was performed using plaster molds. After they had been dried, the samples were pressed at 4 % humidity and 100 MPa in 59 × 14 mm dies. After drying, the samples were fired at 1230 °C and 1400 °C for 1 hour in an electrical furnace, with heating and cooling rate of 5 K/min.

* Corresponding author: e-salahi@merc.ac.ir

Table 1: Chemical and calculated mineralogical analysis of raw materials measured in (wt%).

	SiO ₂	Al ₂ O ₃	K ₂ O	Na ₂ O	CaO	MgO	Fe ₂ O ₃	LOI	K	Q	A	F
SZWNK1	63.5	24.5	0.3	0.4	1.3	0.5	0.5	9	65	28	-	7
Quartz	99.5	0.1	0.05	0.04	0.76	n	0.1	0.1	0	100	-	0
SF11	66.77	17.87	11.51	3.01	0.45	0.1	0.05	0.82	1.1	4.6	-	94.3
Alumina	0.01	98.5	0.55	0.55	0.02	0.02	0.02	1	0	-	100	0

The samples were first verified according to their appearance. The apparent solid and bulk densities and porosity of the samples were measured using the Archimedes method based on the BS 1902 standard. The thermal expansion coefficient of the samples was measured using Netzsch 402E. Polished and HF-etched sections of the bulk materials were analyzed using a S360 Cambridge 1990 scanning electron microscope.

III. Results and discussion

The particle size distribution of the raw materials used is shown in Fig. 1. The appearance of the samples can be categorized in four different states. High-flux-content samples were glassy (shown by G in Figs. 2–6), either at 1230 °C or 1400 °C. As the flux content decreases, the state of the samples changes to become deformed (shown by D), porcelain-like (P), and porous. The numbers in Figs. 2–6 denote the porosity of the samples. Samples with porosity of less than 4 % without deformation were considered as porcelain-like samples. The relationship between the recipe and porosity for 1230 °C is shown in Figs. 2 and 3. Fig. 2 shows the state of the samples in a ternary system (labeled as raw materials) used, as well as the porosity of porous samples. Fig. 3 shows the state of the same samples based on mineralogical content. An obvious map shows the appearance of the samples.

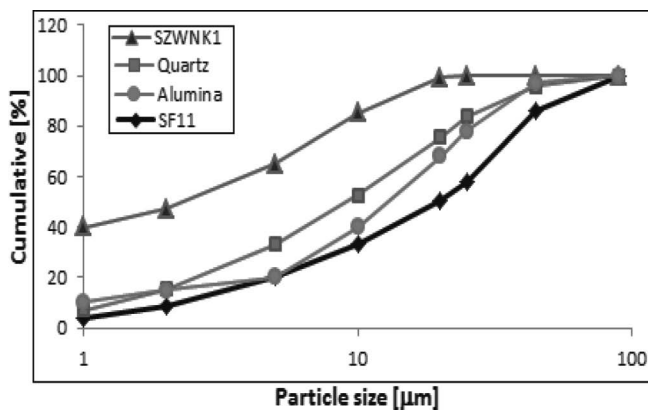


Fig. 1: Particle size distribution of raw materials.

Fig. 4 illustrates the state of the samples and the porosities of the porous samples fired at 1400 °C. The packing of the grains experiences some problems with the high porosity of the samples due to either the low pressure applied, or the non-optimal particle size distribution of raw material. Fig. 5 shows the shrinkage of porous and porcelain-like samples fired at 1230 °C. A number of porous samples (> 10 %) have high shrinkage (> 10 %). The liquid phase formed during firing was not enough to fill the

pores, which in turn shows the influence of the forming process on the final properties of the porcelain obtained.

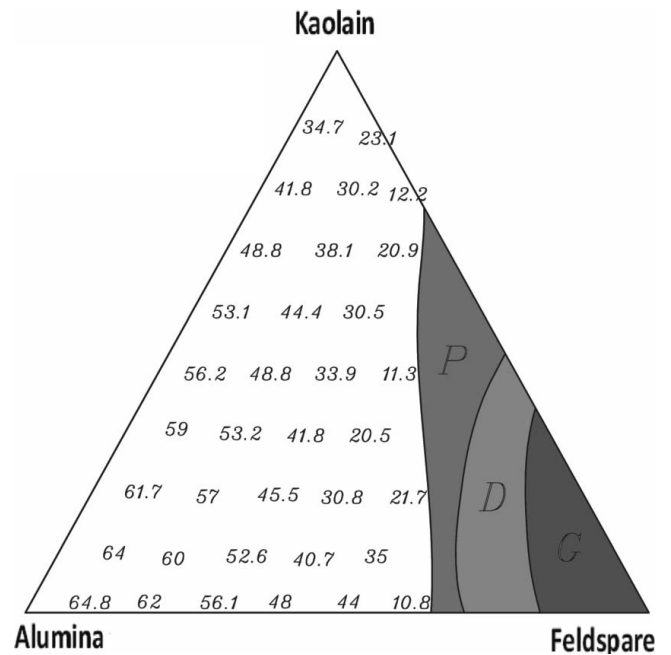


Fig. 2: The state of samples at 1230 °C on raw materials basis. P, D and G denote porcelain-like, deformed and glassy state respectively and numbers are the open porosities (vol%).

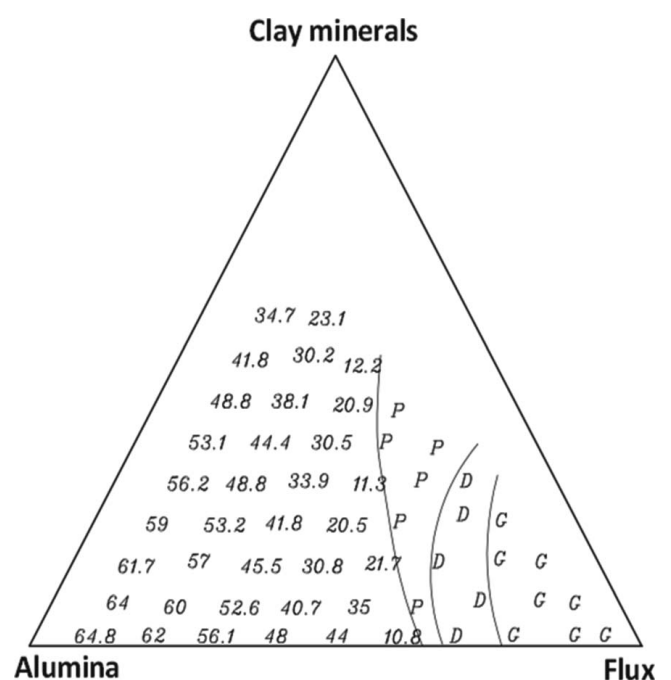


Fig. 3: The state of samples at 1230 °C on mineralogical basis. P, D and G denote like Fig. 2.

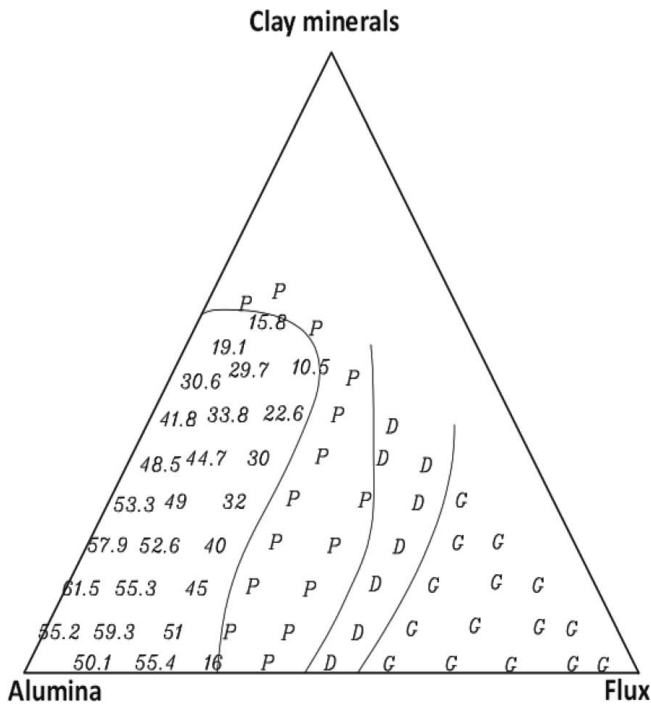


Fig. 4: The state of samples at 1400 °C on mineralogical basis. P, D and G denote like Fig. 2.

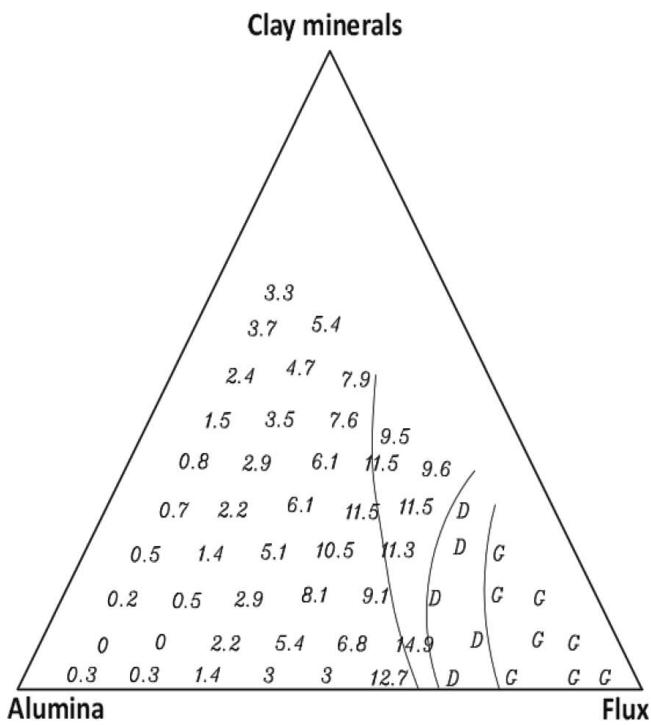


Fig. 5: Linear shrinkage (%) of samples at 1230 °C on mineralogical basis.

This observation can be observed at samples fired at 1400 °C (Fig. 6). Samples with low clay and moderate flux contents have high shrinkage and still remain porous after firing. A comparison between Figs. 3 and 4 reveals that, when the alumina and clay mineral contents in the recipe are equal, the effect of temperature on the reduction of the pores is less significant than when either alumina or clay minerals are less than ~30 %. The curvature of the boundaries changes with increasing firing temperature. All boundaries in Figs. 4 and 5 face to the left and right,

respectively. The region of the glassy samples grows notably and the region of porcelain samples also extends and moves towards alumina (clay mineral side of the diagram). Thus, formulating aluminous porcelains would be easier when the firing temperature is higher. In addition, porcelains with lower flux content can be created when an unfired body has lower porosity. The porosity of green body can be lower when all the parameters of the starting powders, particularly the particle size and size distribution, are optimum. The high porosity of the samples with lower clay content is expected because the similar particle size distribution of alumina and feldspar (Fig. 1) limits the optimum packing of grains.

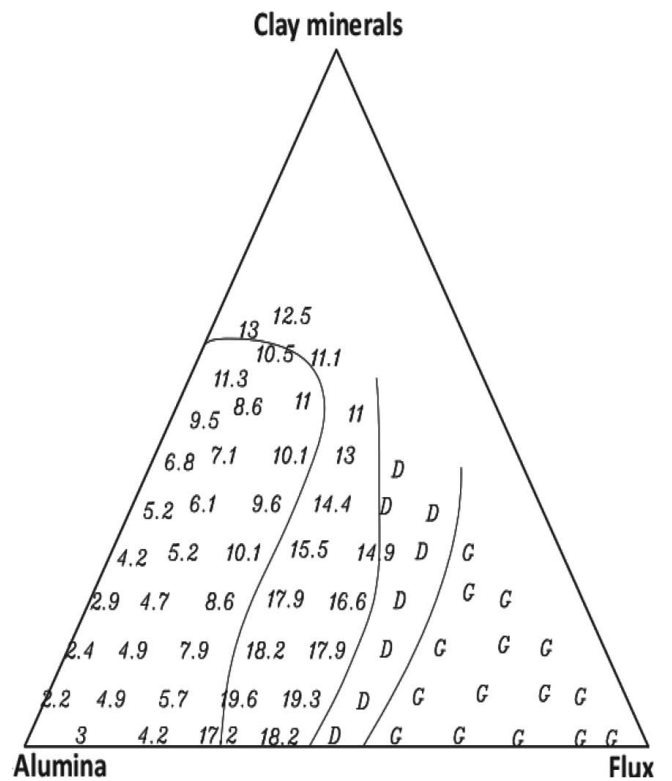
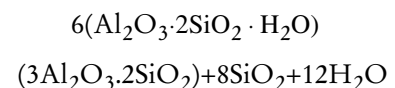


Fig. 6: Linear shrinkage (%) of samples at 1400 °C on mineralogical basis.

Fig. 7 shows the sample compositions mentioned in Table 2. When the amount of flux used is kept constant, more alumina and less clay minerals increase the thermal expansion coefficient at both temperatures studied. The formation of mullite from kaolinite and other clay minerals results in very fine grains of silica according to:



The reduction of thermal expansion by increasing the clay content can be attributed to the dissolution of this silica in the liquid phase formed by the melting of fluxes. Nevertheless, kaolin has silica (Table 1), which can be dissolved in the liquid phase, thereby lowering the thermal expansion. However, the effect of temperature on the thermal expansion of glassy phase is insignificant.

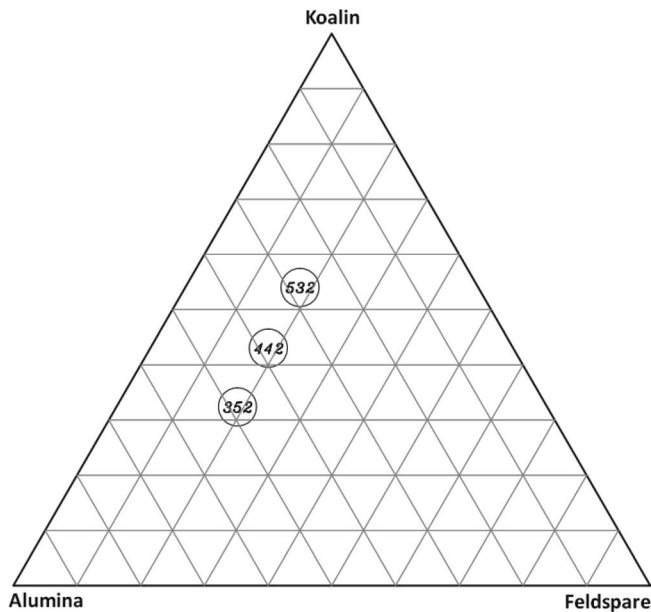


Fig. 7: Composition of samples mentioned in Table 2.

Table 2: Thermal expansion coefficients ($\times 10^6 \text{ K}^{-1}$) of samples with compositions shown in Fig. 7.

Sample No.	T[°C]	
	1400	1230
532	5.3675	5.324
442	5.6506	5.97
352	6.285	6.1451

Using higher firing temperature has no significant effect on the thermal expansion coefficient. Fig. 8 shows the microstructure of sample 442 fired at 1230 °C. The liquid phase did not penetrate into the clay particles. The alumina particles are sintered loosely by the liquid phase. Primary mullite needles are formed in the clay particles with no liquid (Fig. 9). With the increase in temperature, the liquid phase surrounds and dissolves the alumina particles (Fig. 10). In addition, the liquid phase fills the pores and penetrates into the clay particles. As a result, more secondary mullites are formed, as shown in Fig. 11.

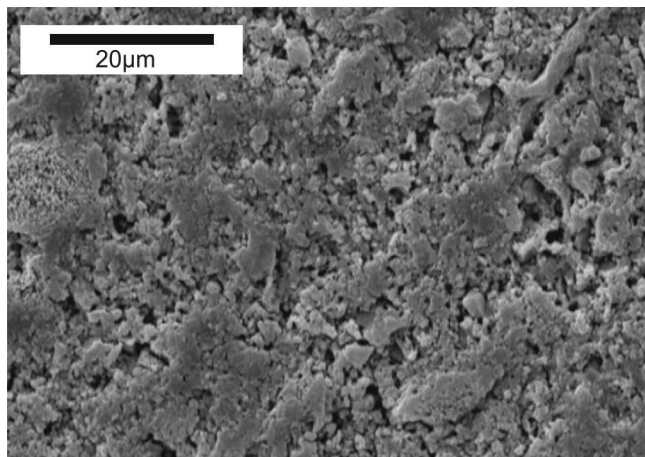


Fig. 8: Sample No. 442 fired at 1230 °C. Etched HF 2 % for 4 min.

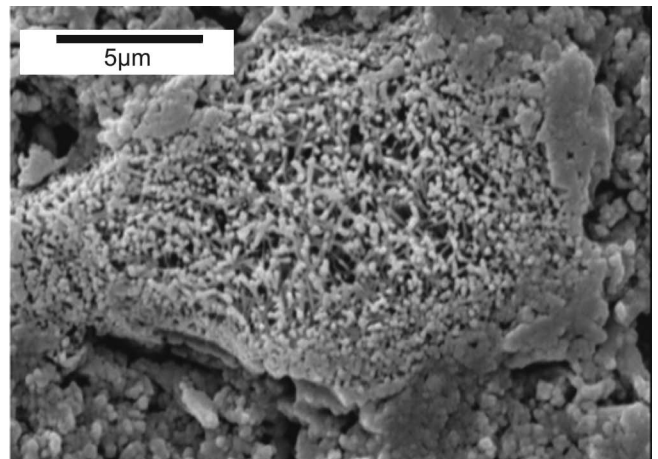


Fig. 9: Primary mullite needles in sample No. 442 fired at 1230 °C. Etched HF 2 % for 4 min.

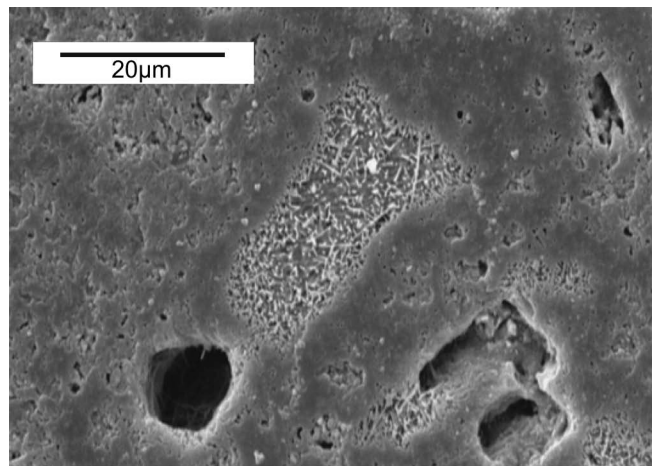


Fig. 10: Sample No. 442 fired at 1400 °C. Etched HF 2 % for 5 min.

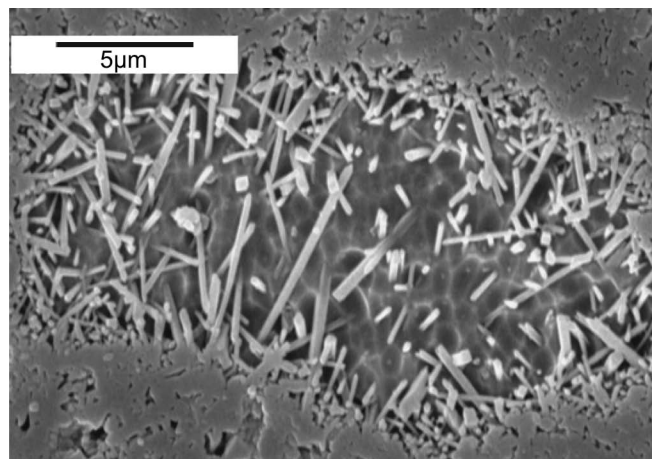


Fig. 11: Secondary mullite needles in sample No. 442 fired at 1400 °C. Etched HF 2 % for 5 min.

IV. Conclusions

According to the experimental results presented and discussed in this paper, the following conclusions can be drawn.

- 1) The mineralogical basis can be used as a method of designing aluminous and siliceous bodies.

- 2) In some circumstances, adding clay helps more to produce dense products than adding flux via better compaction during forming process.
- 3) Increasing the firing temperature widens the composition range of aluminous bodies.
- 4) Bodies with ~ 10 % shrinkage in firing at 1230 °C will result in porcelain-like body. Firing at 1400 °C is accompanied by more shrinkage to produce porcelain bodies. The thermal expansion coefficient of aluminous bodies depends more on the composition than the temperature.

References:

- 1 Stathis, G., Ekonomakou, A., Stournaras, C., Ftikos, C.: Effect of firing conditions, filler grain size and quartz content on bending strength and physical properties of sanitaryware porcelain, *J. Eur. Ceram. Soc.*, **24**, 2357–66, (2004).
- 2 Tarvornpanich, T., Souza, G.P., Lee, W.E.: Microstructural evolution in Clay-Based ceramics I: single components and binary mixtures of clay, flux, and quartz filler, *J. Am. Ceram. Soc.*, **91**, 22, 64–71, (2008).
- 3 Friedrich, A., Wilson, D., Haussühl, E., Winkler, B., Morgenroth, W., Refson, K., *et al.*: High-pressure properties of diasporite, AlO (OH), *Phys. Chem. Miner.*, **34**, 145–57, (2007).
- 4 Štubňa, I., Trník, A., Vozar, L.: Thermomechanical analysis of quartz porcelain in temperature cycles, *Ceram. Int.*, **33**, 1287–91, (2007).
- 5 Demirkesen, E., Erkmen, Z., Yildiz, N.: Effect of Al₂O₃ additions on the thermal expansion behavior of a Li₂O-ZnO-SiO₂ Glass-Ceramic, *J. Am. Ceram. Soc.*, **82**, 3619–21, (1999).
- 6 Dera, P., Lazarz, J.D., Prakapenka, V.B., Barkley, M., Downs, R.T.: New insights into the high-pressure polymorphism of SiO₂ cristobalite. *Phys. Chem. Miner.*, **38**, 517–29, (2011).
- 7 Lima, M., Monteiro, R., Graça, M., Ferreira da Silva, M.: Structural, electrical and thermal properties of borosilicate glass-alumina composites, *J. Alloy. Compd.*, **538**, 66–72, (2012).
- 8 Peternell, M., Hasalová, P., Wilson, C.J., Piazzolo, S., Schulmann, K.: Evaluating quartz crystallographic preferred orientations and the role of deformation partitioning using EBSD and fabric analyser techniques, *J. Struct. Geol.*, **32**, 803–17, (2010).
- 9 Bandyopadhyay, S., Rixecker, G., Aldinger, F., Maiti, H.S.: Effect of controlling parameters on the reaction sequences of formation of nitrogen-containing magnesium aluminate spinel from MgO, Al₂O₃, and AlN, *J. Am. Ceram. Soc.*, **87**, 480–482, (2004).
- 10 Ece, O.I., Nakagawa, Z-E.: Bending strength of porcelains, *Ceram. Int.*, **28**, 131–140, (2002).
- 11 Van Noort, R., Spiers, C., Peach, C.: Structure and properties of loaded silica contacts during pressure solution: impedance spectroscopy measurements under hydrothermal conditions, *Phys. Chem. Miner.*, **38**, 501–516, (2011).
- 12 Maity, S., Sarkar, B.K.: Development of high-strength white-ware bodies, *J. Eur. Ceram. Soc.*, **16**, 1083–1088, (1996).
- 13 Austin, C., Schofield, H., Haldy, N.: Alumina in Whiteware, *J. Am. Ceram. Soc.*, **29**, 341–354, (1946).
- 14 Iqbal, Y., Lee, W.E.: Fired porcelain microstructures revisited, *J. Am. Ceram. Soc.*, **82**, 3584–3590, (1999).
- 15 Carty W.M., Senapati, U.: Porcelain—raw materials, processing, phase evolution, and mechanical behavior, *J. Am. Ceram. Soc.*, **81**, 3–20, (1998).
- 16 Liebermann, J.: Avoiding quartz in alumina porcelain for high-voltage insulators, *Am. Ceram. Soc. Bull.*, **80**, 37–42, (2001).
- 17 Tkalcec, E., Prodanovic, D., Falz, W., Hennicke, H.W.: Microstructure and properties of aluminous electrical porcelain doped with talc, *Brit. Ceram. Trans. J.*, **83**, 76–80, (1984).
- 18 Tkalcec, E., Prodanovic, D., Hennicke, H.W.: Microstructure and properties of aluminous electrical porcelain doped with BaCO₃, *Brit. Ceram. Trans. J.*, **84**, 94–98, (1985).

